

## Supporting Information

### A Diketopyrrolopyrrole-based Macrocyclic Conjugated Molecule for Organic Electronics

By Cheng Li, Chao Wang, Yiting Guo, Yingzhi Jin, Nannan Yao, Yonggang Wu, Fengling Zhang and Weiwei Li\*

#### Contents

1. Photovoltaic and OFET devices fabrication
2. Field effect mobilities
3. Solar cells performance
4. <sup>1</sup>H-NMR, <sup>13</sup>C-NMR and mass spectrum

#### 1. Photovoltaic and OFET devices fabrication

Photovoltaic devices with inverted configuration were made by spin-coating a ZnO sol-gel at 4000 rpm for 60 s onto pre-cleaned, patterned ITO substrates. The photoactive layer was deposited by spin coating a chloroform solution containing the P3HT and **C-DPP** and the appropriate amount of *o*-DCB as processing additive in air. MoO<sub>3</sub> (10 nm) and Ag (100 nm) were deposited by vacuum evaporation at ca.  $4 \times 10^{-5}$  Pa as the back electrode. The P3HT:**L-DPP** films were spin coated at 130 °C from 1,1,2,2-tetrachloroethane solution. The active area of the cells was 0.04 cm<sup>2</sup>. The *J-V* characteristics were measured by a Keithley 2400 source meter unit under AM1.5G spectrum from a solar simulator (Enlitech model SS-F5-3A). Solar simulator illumination intensity was determined at 100 mW cm<sup>-2</sup> using a monocrystal silicon reference cell with KG5 filter. Short circuit currents under AM1.5G conditions were estimated from the spectral response and convolution with the solar spectrum. The external quantum efficiency was measured by a Solar Cell Spectral Response Measurement System QE-R3011 (Enli Technology Co., Ltd.). The thickness of the active layers in the photovoltaic devices was measured on a BRUKER Dektak XT profilometer.

The organic field-effect transistors were fabricated on a commercial Si/SiO<sub>2</sub>/Au substrate purchased from First MEMS Co. Ltd. A heavily N-doped Si wafer with a SiO<sub>2</sub> layer of 300 nm served as the gate electrode and dielectric layer, respectively. The Ti (2 nm)/Au

(28 nm) source–drain electrodes were sputtered and patterned by a lift-off technique. Before deposition of the organic semiconductor, the gate dielectrics were treated with octadecyltrichlorosilane (OTS) in a vacuum oven at a temperature of 120 °C, forming an OTS self-assembled monolayers. The treated substrates were rinsed successively with hexane, chloroform, and isopropyl alcohol. Polymer thin films were spin coated on the substrate from solution with a thickness of around 30 – 50 nm. The devices were thermally annealed at 150 °C for 10 min in a glovebox filled with N<sub>2</sub>. The devices were measured on an Keithley 4200 SCS semiconductor parameter analyzer at room temperature. The mobilities were calculated from the saturation region with the following equation:  $I_{DS} = (W/2L)C_i\mu(V_G - V_T)^2$ , where  $I_{SD}$  is the drain–source current,  $W$  is the channel width (1400  $\mu\text{m}$ ),  $L$  is the channel length (50  $\mu\text{m}$ ),  $\mu$  is the field-effect mobility,  $C_i$  is the capacitance per unit area of the gate dielectric layer, and  $V_G$  and  $V_T$  are the gate voltage and threshold voltage, respectively. This equation defines the important characteristics of electron mobility ( $\mu$ ), on/off ratio ( $I_{\text{on}}/I_{\text{off}}$ ), and threshold voltage ( $V_T$ ), which could be deduced by the equation from the plot of current–voltage.

## 2. Field effect mobilities

**Table S1.** Field effect mobilities of **C-DPP** in a BGBC configuration. The thin films were spin-coated from CHCl<sub>3</sub>/n-hexane (10%).

	TA [°C]	$\mu_h$ [cm <sup>2</sup> V <sup>-1</sup> s <sup>-1</sup> ]	$V_T$ (V)	$I_{\text{on}}/I_{\text{off}}$	$\mu_e$ [cm <sup>2</sup> V <sup>-1</sup> s <sup>-1</sup> ]	$V_T$ (V)	$I_{\text{on}}/I_{\text{off}}$
<b>C-</b>	RT	2.3×10 <sup>-4</sup>	-4.0	6×10 <sup>3</sup>	2.3×10 <sup>-4</sup>	74.5	7×10 <sup>2</sup>
<b>DPP</b>	150	3.4×10 <sup>-3</sup>	-4.4	1×10 <sup>6</sup>	4.7×10 <sup>-6</sup>	73.4	3×10 <sup>1</sup>

## 3. Solar cells performance

**Table S2.** Characteristics of P3HT:**C-DPP** solar cells spin coated from different solvent. The ratio of donor to acceptor was 1:1. The thickness of active layers was around 80 nm.

Solvent	$J_{\text{sc}}^a$ [mA/cm <sup>2</sup> ]	$V_{\text{oc}}$ [V]	FF	PCE [%]
CF	1.26	0.66	0.32	0.27
CF/DIO (2%)	0.83	0.60	0.39	0.19
CF/ <i>o</i> -DCB (10%)	1.23	0.69	0.44	0.37

**Table S3.** Characteristics of P3HT:**C-DPP** solar cells spin coated from different ratio of donor to acceptor in CF/*o*-DCB (10%). The thickness of active layers was around 80 nm.

Ratio	$J_{sc}^a$ [mA/cm <sup>2</sup> ]	$V_{oc}$ [V]	FF	PCE [%]
2:1	0.60	0.65	0.41	0.16
1:1	1.23	0.69	0.44	0.37
1:2	0.92	0.67	0.40	0.25

**Table S4.** Characteristics of P3HT:**C-DPP** solar cells spin coated from CF/*o*-DCB (10%) with different annealing temperature. And the ratio of donor to acceptor was 1:1. The thickness of active layers was around 80 nm.

Annealing temperature [°C]	$J_{sc}^a$ [mA/cm <sup>2</sup> ]	$V_{oc}$ [V]	FF	PCE [%]
RT	1.23	0.69	0.44	0.37
150	1.65	0.67	0.44	0.49
200	1.20	0.78	0.43	0.40

**Table S5.** Characteristics of P3HT:**C-DPP** solar cells with different thickness spin coated from CF/*o*-DCB (10%) annealed at 150 °C . And the ratio of donor to acceptor was 1:1.

Thickness [nm]	$J_{sc}^a$ [mA/cm <sup>2</sup> ]	$V_{oc}$ [V]	FF	PCE [%]
51	1.47	0.68	0.47	0.46
79	1.65	0.67	0.44	0.49
106	1.30	0.67	0.41	0.35

**Table S6.** Photovoltaic performances of 10 devices based on P3HT:**C-DPP** (1:1) fabricated from CF/*o*-DCB (10%).

No.	$J_{sc}$ [mA/cm <sup>2</sup> ]	$V_{oc}$ [V]	FF	PCE [%]
1	1.47	0.68	0.47	0.46
2	1.57	0.68	0.44	0.47
3	1.56	0.67	0.41	0.43
4	1.65	0.67	0.44	0.49

5	1.51	0.67	0.45	0.45
6	1.56	0.67	0.41	0.43
7	1.49	0.68	0.43	0.44
8	1.50	0.68	0.44	0.45
9	1.54	0.68	0.43	0.45
10	1.56	0.66	0.39	0.40
average	$1.54 \pm 0.052$	$0.67 \pm 0.007$	$0.43 \pm 0.023$	$0.45 \pm 0.025$

#### 4. $^1\text{H-NMR}$ , $^{13}\text{C-NMR}$ and mass spectrum.

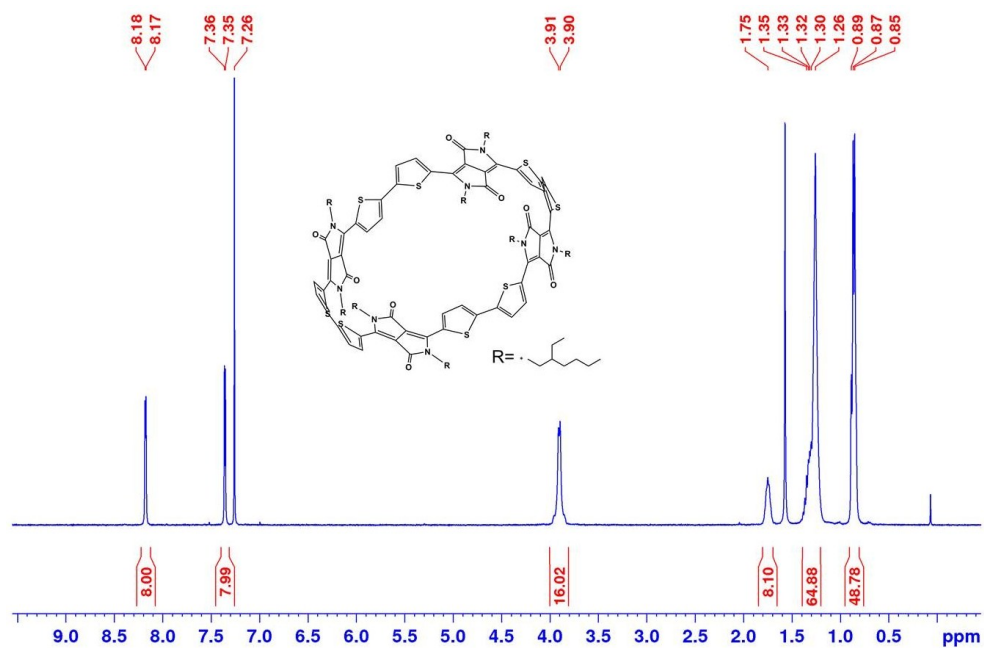
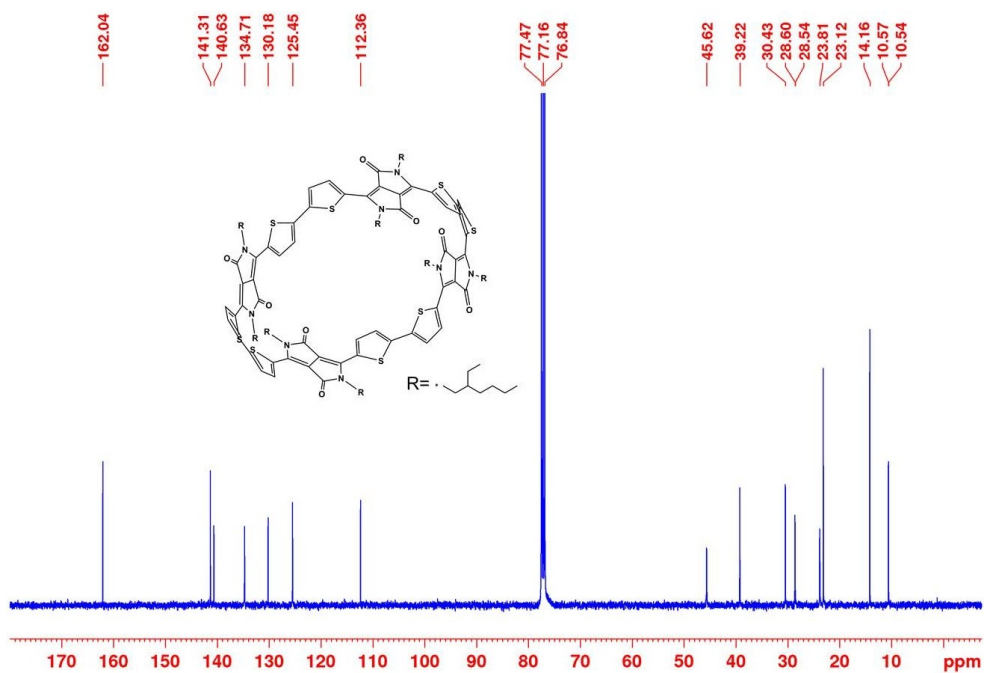
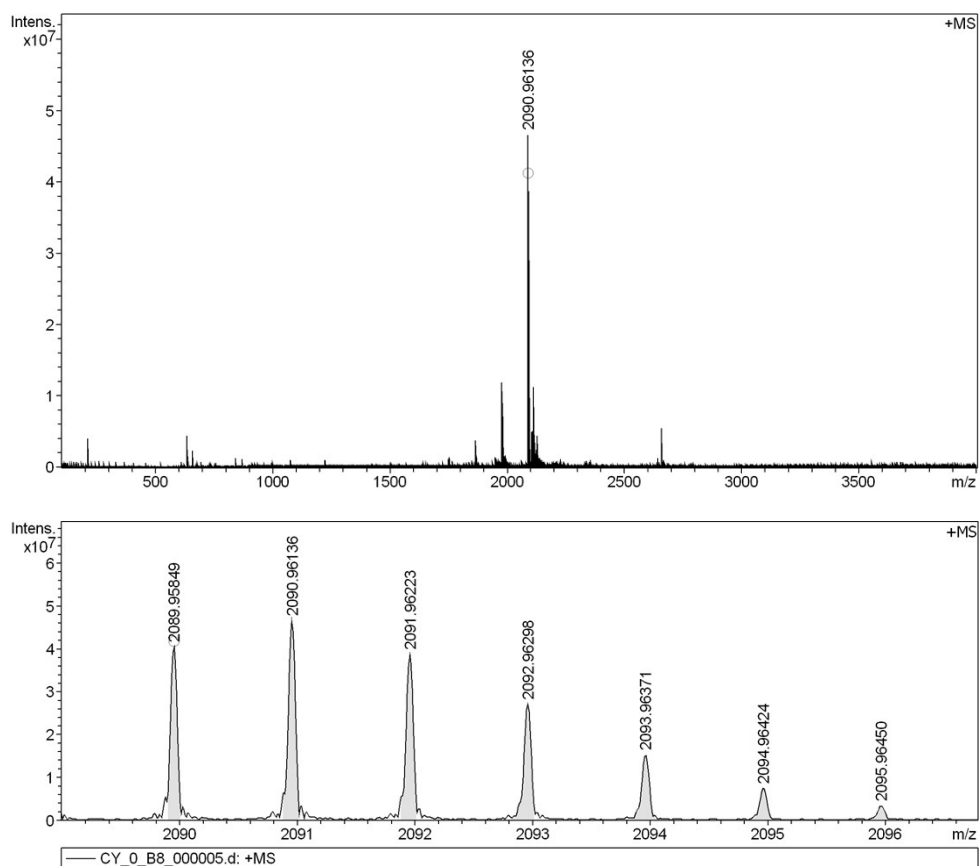


Figure S1.  $^1\text{H-NMR}$  of C-DPP in  $\text{CDCl}_3$ .



**Figure S2.**  $^{13}\text{C}$ -NMR of C-DPP in  $\text{CDCl}_3$ .



**Figure S3.** HRMS of C-DPP.

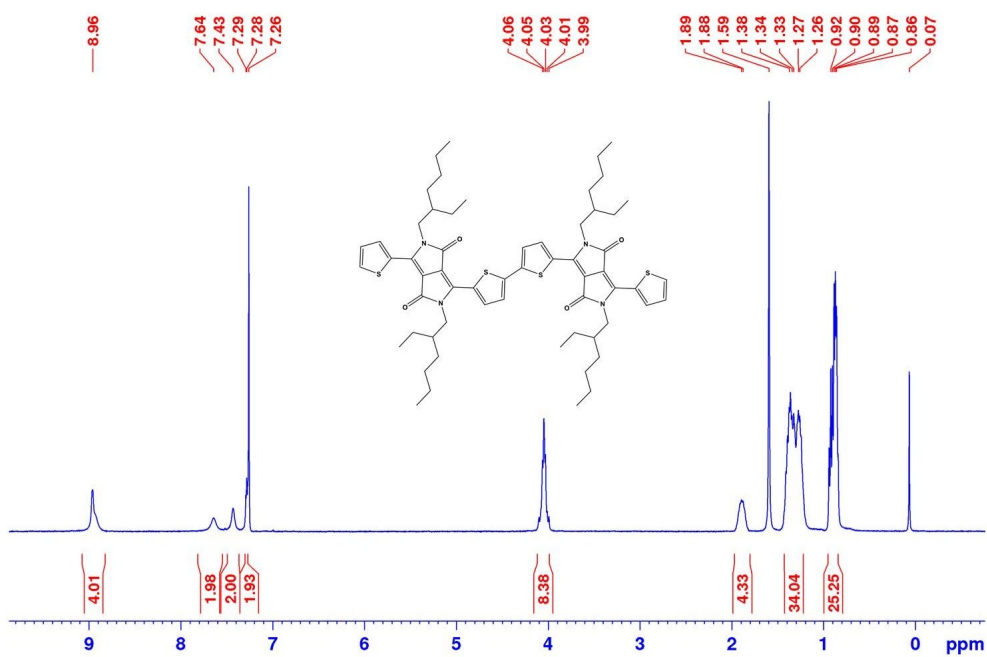


**Figure S4.**  $^1\text{H}$ -NMR of compound **4** in  $\text{CDCl}_3$ .

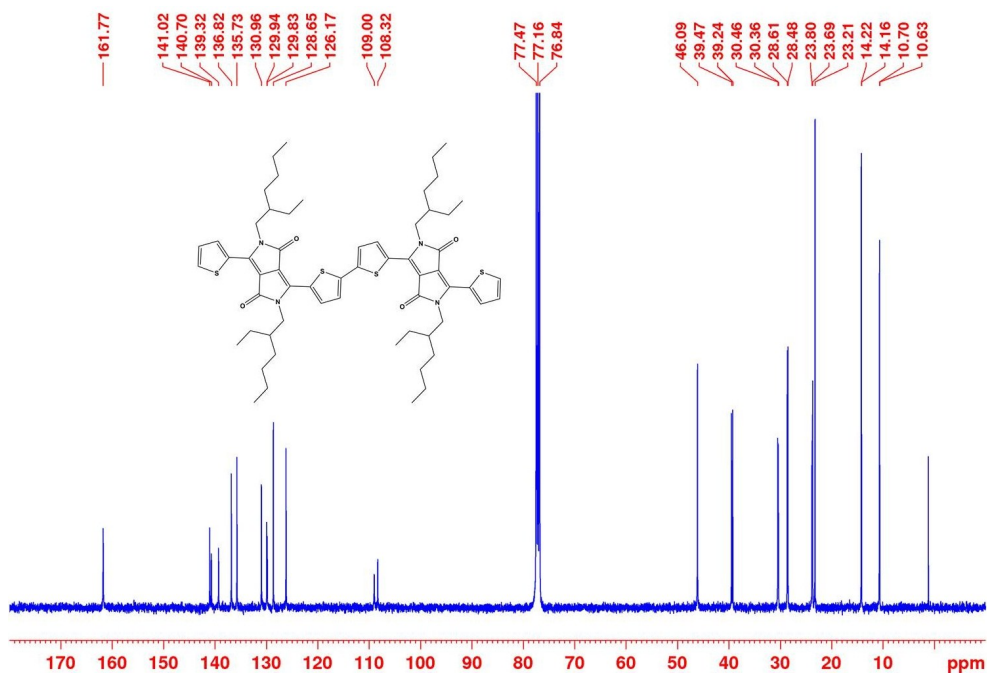


Figure S5.  $^{13}\text{C}$ -NMR of compound 4 in  $\text{CDCl}_3$ .

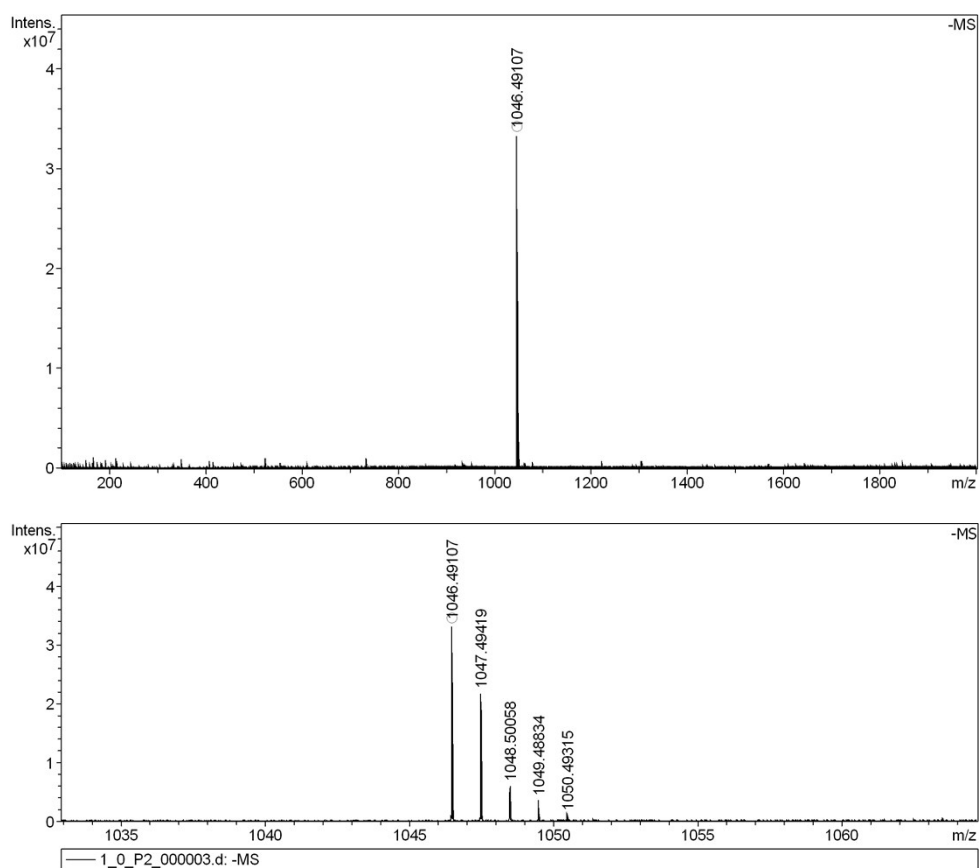


Figure S6. HRMS of compound 4.

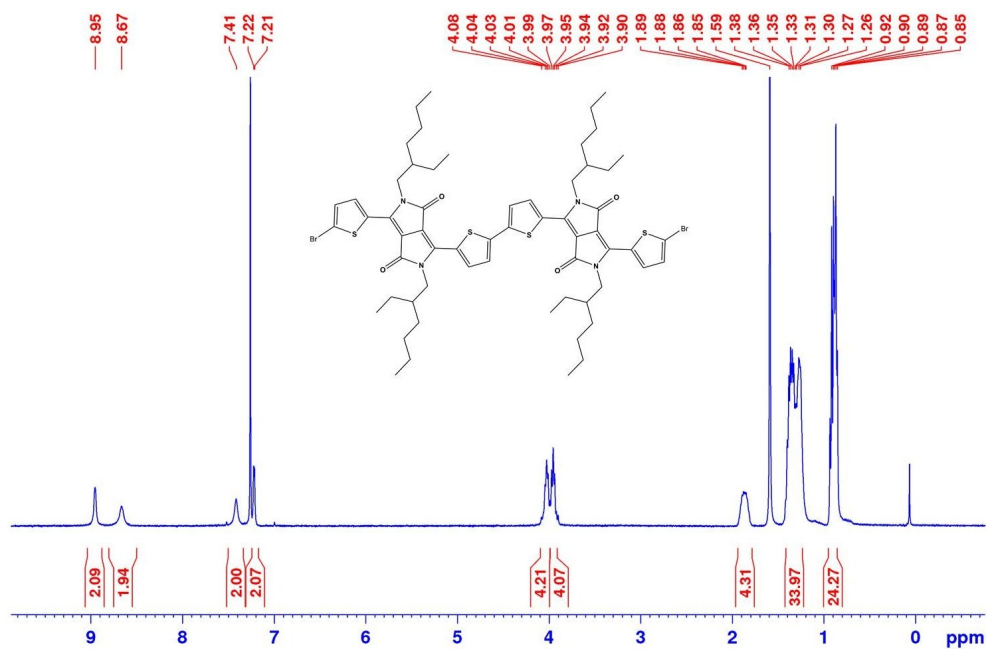


Figure S7. <sup>1</sup>H-NMR of compound 5 in CDCl<sub>3</sub>.

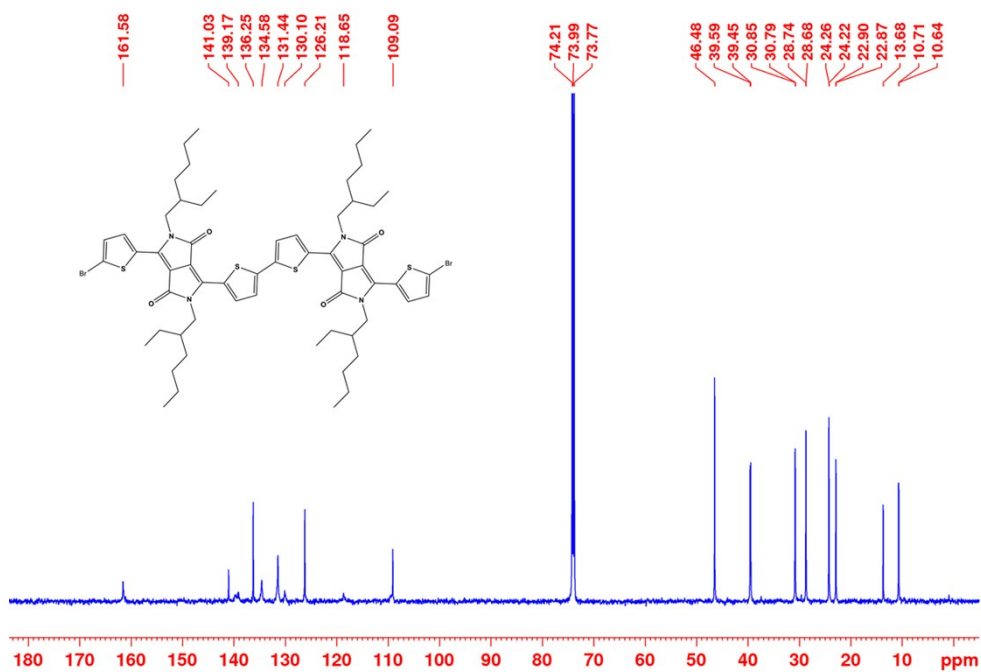
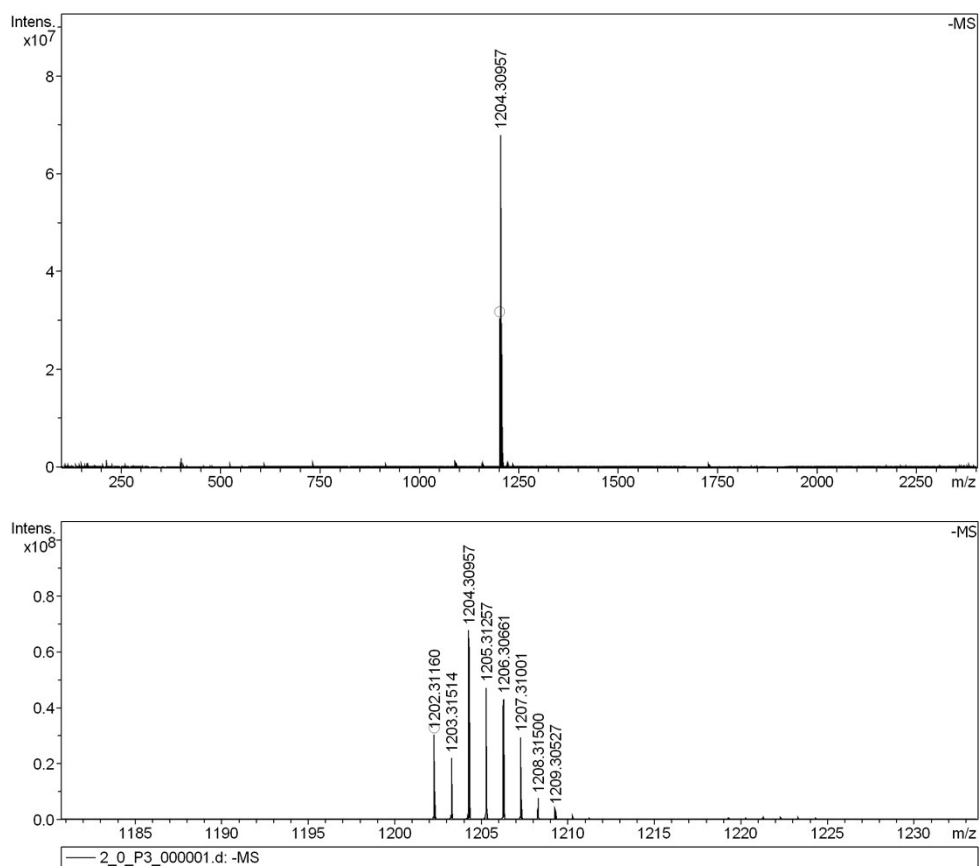
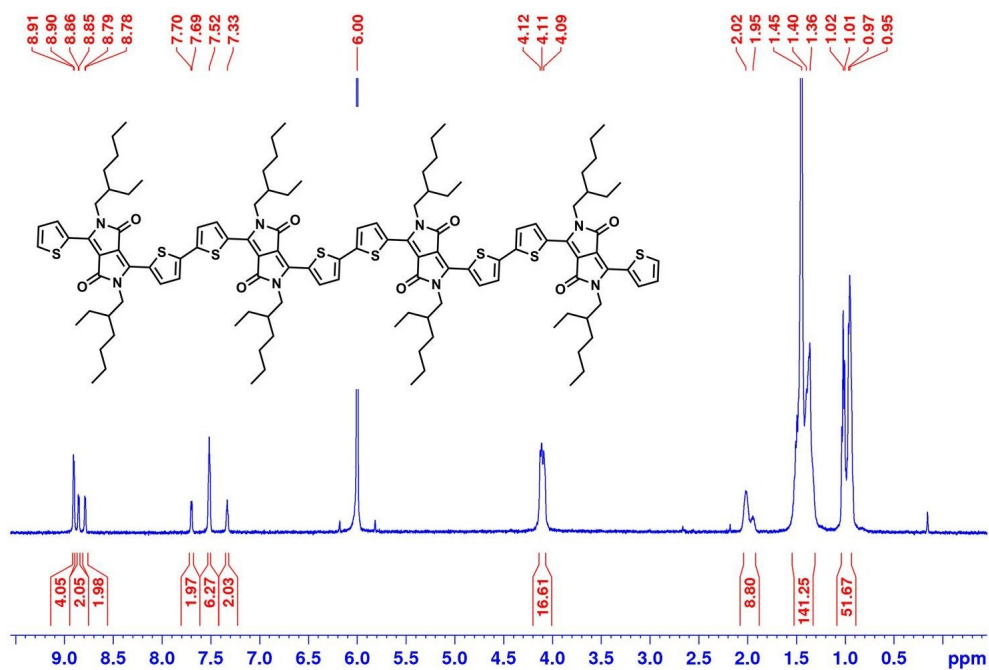


Figure S8. <sup>13</sup>C-NMR of compound 5 in 1,1,2,2-tetrachloroethane-D<sub>2</sub> at 100 °C, 500MHz.



**Figure S9.** HRMS of compound 5.



**Figure S10.** <sup>1</sup>H-NMR of L-DPP in 1,1,2,2-tetrachloroethane-D<sub>2</sub> at 100 °C, 500MHz. Signals around 1.45 ppm overlap with the signal of H<sub>2</sub>O.



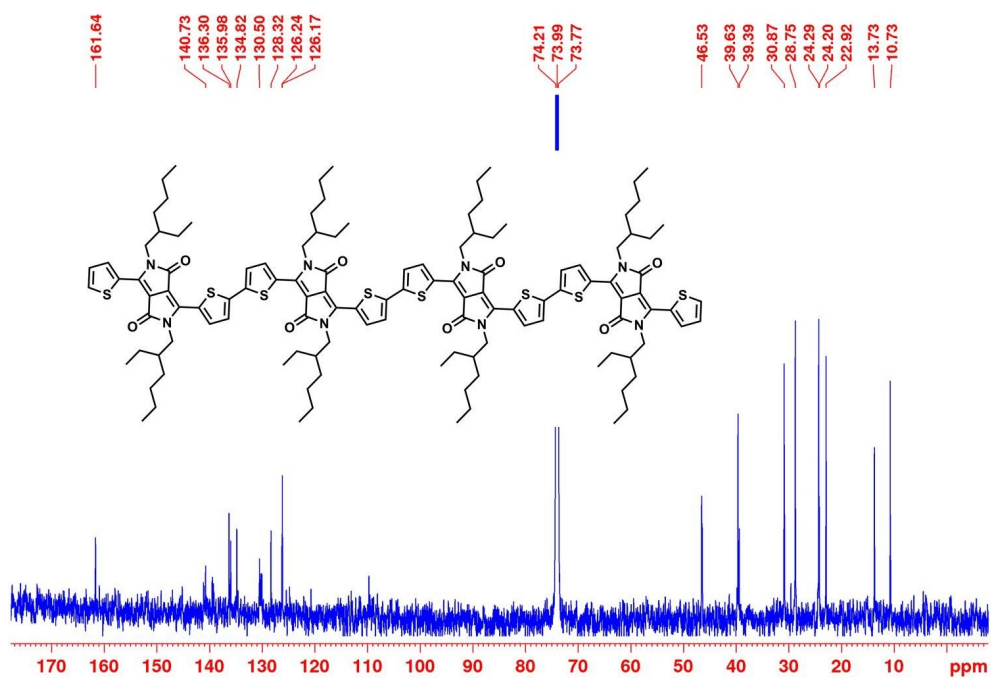


**Figure S11.**  $^{13}\text{C}$ -NMR of L-DPP in 1,1,2,2-tetrachloroethane- $\text{D}_2$  at 100 °C, 500MHz

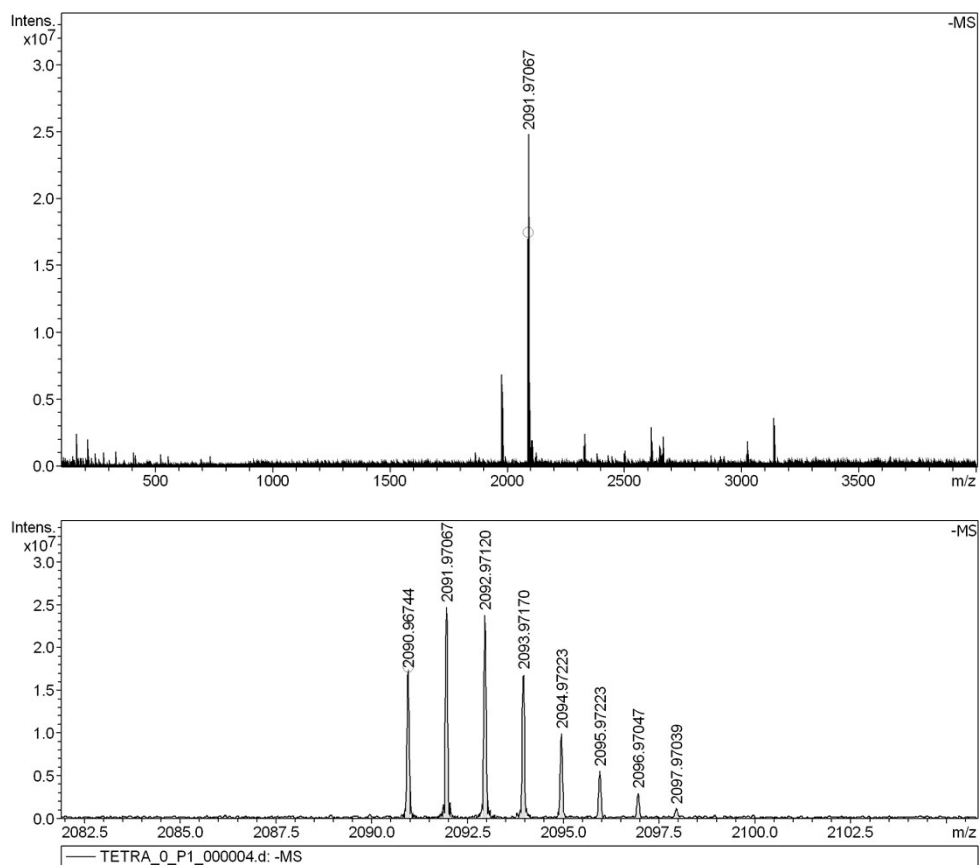


**Figure S12.** HRMS of L-DPP.